ELSEVIER

Catalysis Today 39 (1997) 145–157

CATALYSIS TODAY

At the time he made the first photographs on paper: Did Henry Fox Talbot oxidize water to oxygen with sunlight?

Gion Calzaferri[1]

Department of Chemistry and Biochemistry, University of Bern, Freiestrasse 3, CH-3000 Bern, Switzerland

Abstract

Photocatalytic water oxidation to O_2 takes place at the solid/water phase boundary of an appropriately prepared thin AgCl layer in the presence of a small excess of Ag^+. This water oxidation reaction shows self-sensitization: as the reaction proceeds, the sensitivity is extended from the near-UV–visible towards the red range. This means that new photo active colour centres are formed upon near UV illumination composed of reduced silver species. The quantum yield per redox equivalent for O_2 evolution upon illumination with near UV light (340–390 nm) is ~0.8 and it is the same upon illumination with blue light (420–480 nm). In the green range it is ~0.5. We discuss parameters controlling these reactions. Some of our observations parallel those made by Henry Fox Talbot 160 years ago when he made his first "photogenic drawings" on silver chloride containing paper.

Zeolite microcrystals are investigated as hosts for supramolecular organization of clusters, complexes and molecules. They offer possibilities to design precise and reversible functionalities which have the potential to become useful in a solar energy conversion system because in favourable cases very stable materials have been obtained. The possibility to arrange zeolite microcrystals of good quality and narrow size distribution as dense monograin layers on different types of substrates allows the discovery of specific properties. In the present context, three functionalities are of special importance: intrazeolite ion transport, intrazeolite charge transport and intrazeolite excitation energy transport. All of them have been clearly demonstrated experimentally although there are still some controversies going on. The zeolite acts as a host in each case mentioned. It is not actively involved in the corresponding processes, but provides the necessary geometrical and chemical environment.

Favourable conditions for finding an efficient antenna device are a high concentration of monomeric dye molecules with a large Förster energy transfer radius, high luminescence quantum yield and ideal geometrical arrangement of the chromophores, as well as an optimal size of the device. Very interesting supramolecular devices can be realized by enclosing dyes inside a microporous material such that the volume of the cages and channels is able to uptake monomers only, but not aggregates.

Keywords: Photocatalytic water oxidation; Zeolite microcrystals; Ag^+/AgCl layers

1. Introduction

An important aim of photochemistry is to discover or to design structurally organized and functionally integrated artificial systems which are capable to elaborate the energy and information input of photons to perform functions which are useful for energy or information purposes. In natural photosynthesis, light is absorbed by an antenna system of a few hundred chlorophyll molecules arranged in a protein environ-

[1]Tel.: +46-31-631-4236; Fax: +46-31-631-3994

0920-5861/97/$32.00
PII S0920-5861(97)00096-5

ment which allows a fast energy transfer from an electronically excited molecule to unexcited neighbour molecules in a way that the excitation energy reaches the reaction centre with high probability. Trapping occurs there. An artificial antenna system is an organized multicomponent arrangement in which several chromophoric molecular species absorb the incident light and channel the excitation energy (not charges) to a common acceptor component [1]. Experiments for controlled transport of excitation energy through thin layers based on Langumuir–Blodgett films have been described many years ago by Kuhn and coworkers [2]. Some sensitization processes in silver halide photographic materials and also the "dyes, complexes and thin layers in sensitization solar cells" [3] bear in some cases aspects of artificial antenna systems [4].

An overview of relevant processes in a photochemical water splitting device in which the oxidation of water to oxygen and its reduction to hydrogen are separated by a membrane is illustrated on the upper part of Fig. 1. Water oxidation takes place at the solid/liquid phase boundary. An antenna absorbs and transports the excitation energy to an oxidizing species which is itself reduced. Reoxidation takes place by electron transport to the membrane and then through it to the reducing side. Using a mediator for transporting the electron to the reducing species at the phase boundary where hydrogen evolution takes place is an interesting possibility. Realizing such a device in which several parts play well together is the aim but it is indeed a demanding task. A conceptual simplification can be made by substituting the membrane temporarily by two electrodes as illustrated on the lower part of Fig. 1. This allows to study the oxidative and the reductive parts separately. We refer to [5,6] for recent reviews on photochemical water splitting.

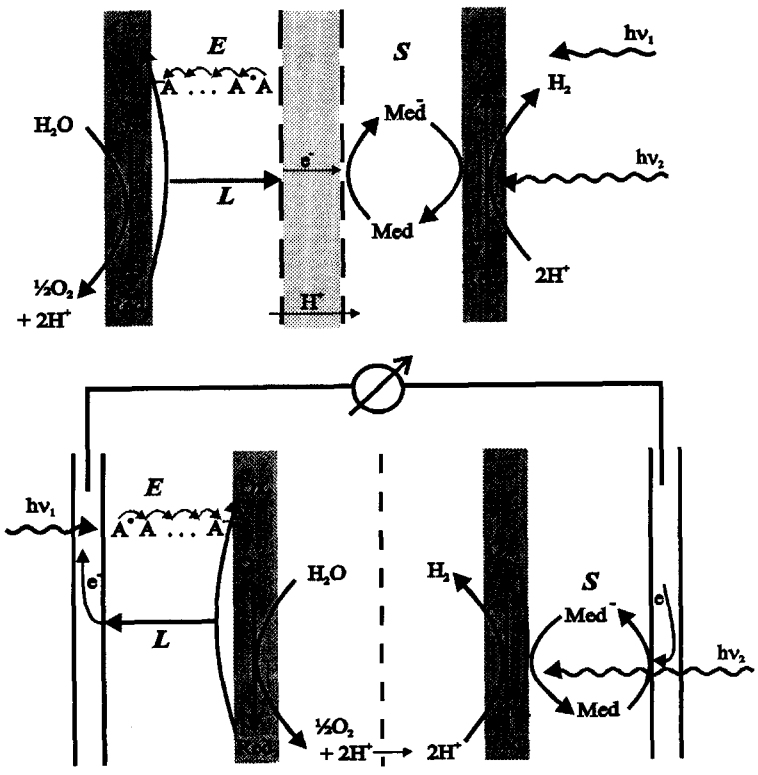

Fig. 1. Overview of relevant processes in a photochemical water splitting device. Upper part: The oxidation of water to oxygen and its reduction to hydrogen are separated by a membrane. Lower part: Simplification by substituting the membrane by two electrodes. *E* indicates migration of excitation energy, *L* indicates charge transport and *S* indicates charge transport by a mediator.

We have focused on three problems: the water oxidation in absence of an externally added potential, the charge transport in an organized microporous media and the transport of excitation energy in an antenna system. I will start by discussing the photocatalytic oxidation of water on Ag^+ containing systems and the self-sensitization taking place during this reaction. A few remarks on zeolite microcrystals as hosts for supramolecular organization of clusters, complexes and molecules will then lead to an actually promising project concerning the energy transfer between dye molecules in the nanopores of hexagonal microcrystals.

I became interested in the water oxidizing ability of Ag^+–A zeolite containing systems when we observed that self-sensitization takes place: as the reaction proceeds, the sensitivity is extended from near-UV–visible wavelengths towards the red range [7–9]. We recently examined the influence of Cl^- on this reaction [10] and we found that thin AgCl layers evolve O_2 in the presence of a small excess of Ag^+ ions. This system shows the same type of self-sensitization as we reported earlier. The quantum yield for O_2 evolution upon illumination with near UV light is ~0.8 and it is the same upon illumination with blue light (420–480 nm). In the green range (500–540 nm) it is ~0.5. If this system is to become useful in a regenerative way, the reduced silver species must be reoxidized to silver cations in a completely reversible process. Recent photoelectrochemical experiments on Ag^+/AgCl layers on conduction SnO_2 and on other electrodes gave encouraging results in that simultaneous photocatalytic oxygen generation from water and oxidation of the reduced silver could be observed over many hours [11].

Zeolite microcrystals offer the possibility to act as hosts for supramolecular organization of cluster complexes and molecules. One can imagine that such an organized system should allow to design precise and reversible functionalities which have the potential to become useful in a solar energy conversion system. As an example, the electronic structure of silver zeolite A is very interesting and offers possibilities for building new devices. Very different systems are obtained by intercalating strongly luminescent organic dyes such as pyronine, oxonine and others into the channels of zeolite L and other hexagonal zeolites with channel structure. The geometrical constraints of this system excludes aggregation and therefore self-quenching up to very high concentrations of about 0.2 M. The highly anisotropic arrangement realized in such systems has been used to study possibilities for building an efficient light harvesting antenna system based on Förster energy transfer. The principle of such a device is illustrated in Fig. 2. We have shown that its pronounced anisotropy strongly favours the probability to reach a trap located in the middle of one of the ends of the cylinder shaped microcrystals [12].

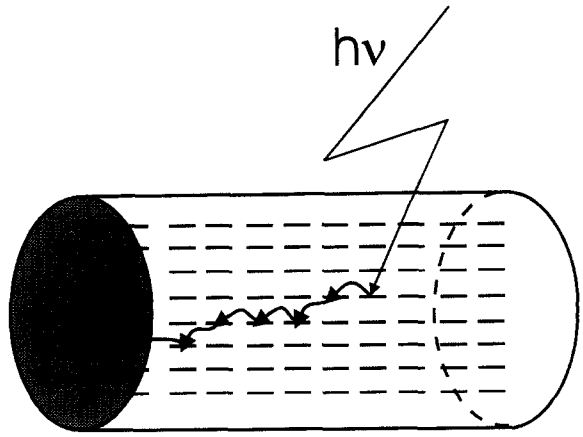

Fig. 2. An artificial antenna system. Light is collected and absorbed by the dye molecules indicated as bars. The direction of the transition of the first electronic transition coincides with the axis of the cylinder. The excitation then migrates along the linearly arranged dye molecules until it reaches the trap, marked by a star, as indicated by the arrows. An important aspect of this device is its pronounced anisopropy concerning the excitation energy migration.

2. At the time he made the first photographs on paper – did Henry Fox Talbot oxidize water to oxygen with sunlight?

The photochemical oxidation of water to oxygen is a four-electron process. It is therefore intrinsically difficult to understand. In green plants it is assumed to proceed via a manganese complex system but despite intense research many open questions remain to be answered [13,14]. Remarkably interesting chemistry has been developed in attempts to mimic the natural systems but it seems that there is still a very long way to go before we reach this goal.

The photographing papers of Henry Fox Talbot, prepared around 1834, were made by first soaking in sodium chloride solution and then brushing with an excess of silver nitrate solution. The key to success was the observation that the paper was more sensitive to light where there was a deficiency of NaCl [15]. We recently reported that the photochemical oxygen evolution of a silver chloride containing zeolite in presence of water depends on the added amount of Cl^- [10,16]. We found that there is a maximum of O_2 production where there is a deficiency of Cl^- with respect to stoichiometric AgCl. I became aware of the fact that our observations parallel those made by Talbot 160 years ago when I followed a paper presented by Dr. Ware at the IS and T's 48th Annual Meeting in Washington 1995 [17]. Since then I assume that the first photographic papers of Talbot were based on the ability of silver chloride to oxidize water to oxygen with high quantum yield in presence of an excess of Ag^+ ions. These early silver photographs were not fixed by thiosulphate but were simply "stabilized" by an excess of halide ions. Talbot published an article entitled "The Nature of Light" in 1835 in which he described an observation that resembles the *latent image* formation which made silver photography so successful and which was close to the *self-sensitization process* for the photochemical oxidation of water, discovered by us a few years ago [7–10,16]. Talbot did not understand what he had observed but the description of the phenomenon is remarkably precise. He writes: "...A sheet of paper was moistened with a solution of nitrate of silver, a substance which, it is well known, is capable of being blackened by the influence of solar light. Half of the paper was covered, and half exposed to sunshine; but owing to its being a dull day in the winter season, no effect was produced. After several minutes the paper was removed, and being examined, showed hardly any perceptible difference between the part that had been covered and that which had been exposed to the sun. It was then removed to another room, where the sun does not shine in the winter season, and accidentally exposed to daylight. Some hours afterwards I was surprised to find that the paper had become partially darkened, and that the dark part was that which had been previously but ineffectually exposed to the sunshine, while the other part still retained much of its original whiteness. This anomalous fact, of which I could find no explanation at the time, appears to me now to be closely connected with what I have advanced as a probable cause of phosphorescence...".

The three essential observations made by Talbot that (i) his paper was more sensitive to light where there was a deficiency of NaCl; (ii) that his paper could be "stabilized" by an excess of Cl^- under optimized conditions and (iii) that it could be sensitized by moderate illumination parallel to important observations we have made when studying the ability of Ag^+ containing systems in the presence of a deficiency of Cl^- to photo-oxidize water to oxygen [10,16].

Baur and Rebmann [18] seem to be the first to report on minor O_2 evolution from water on UV illumination of AgCl. An article of Vogel [19] dating back to 1863 which is sometimes wrongly referred as to be the first report on photochemical O_2 production from AgCl does not contain any hints on photochemical O_2 evolution. Vogel was probably, however, the first to demonstrate the photochemical oxidation of Cl^- to Cl_2 in an aqueous silver chloride system which at the same time became more acidic on illumination with sunlight under certain conditions. In a study of the pH dependence of the photochemical properties of AgCl and of Ag^+–A zeolite, both in the presence of a large excess of Cl^-, we have shown that, under acidic conditions, Cl_2 is evolved with a significant quantum yield and O_2 signals appear only in the strongly alkaline region. We also found that this system shows self-sensitization. Based on these observations we built an $\{Ag^+/AgCl\|Cl^-/Cl_2\}$ photogalvanic cell with an open circuit potential of 1.05 V, but poor power/voltage behaviour [20,21].

Metzner and coworkers reinvestigated the experiments of Baur and Rebmann in an attempt to contribute to the understanding of the ability of the natural photosystem II to evolve oxygen. They observed significant O_2 evolution from AgCl suspensions containing an excess of Ag^+ showing a maximum of sensitivity at about pH 5 [22,23]. Chandrasekaran and Thomas [24] observed photochemical oxidation of water with AgCl in the presence of an excess of Ag^+ with a low quantum yield but they did not try to optimize the conditions. They assumed that OH-radicals play a role in this process but no evidence was advanced to support this. We have a good reason to believe that these radicals do not play any role in the photocatalytic oxidation of water by $AgCl/Ag^+$

systems. This is consistent with the finding of Taube and Bray [25] that OH-radicals react with chloride to form Cl-radicals.

We conclude that the observations (i) and (ii) of Talbot were repeated with partial success in a number of laboratories over several decades by experimentalists not being aware of it, however.

I became interested in the water oxidizing ability of Ag^+–A zeolite containing systems, contaminated with some AgCl, when we observed that a system that has never been exposed to near UV light (~370 nm) is insensitive to visible light but that it becomes sensitive and is capable to photo-oxidize water to O_2 in the whole visible range with a limit between 600 and 700 nm with high quantum yield under optimized conditions. We named this a "self-sensitization process", because as the reaction proceeds, the sensitivity is extended from the near UV wavelengths towards the red range [7–10,16]. The self-sensitization parallels the observation (iii) described by Talbot in 1835.

Our present knowledge on the ability of Ag^+ containing systems in presence of an optimal amount of Cl^- to photo-oxidize water to oxygen can be summarized as follows:

1. $AgCl/Ag^+$ on zeolites, on SnO_2, on glass, on silver, and on other substrates is able to photocatalytically-oxidize water to O_2 according to the following stoichiometry:

$$[n\mathrm{Ag}^+, m\mathrm{AgCl}] + \frac{r}{2}\mathrm{H_2O} \xrightarrow{h\nu} [(n-r)\mathrm{Ag}^+, m\mathrm{AgCl}, r\mathrm{Ag}^0] + r\mathrm{H}^+ + \frac{r}{4}\mathrm{O_2}$$

   Important parameters are: the Ag^+ to Cl^- ratio, the pH, the wavelength and the light intensity.
2. Self-sensitization occurs under all conditions investigated. A system that has never been exposed to light is insensitive to the visible part of the spectrum: After it has been once irradiated in the near UV it becomes sensitive and is capable to photo-oxidize water in the whole visible range with a lower limit between 600 and 700 nm. Once the system has been sensitized, the near UV irradiation can be omitted.
3. The oxygen evolution rate is not linear at low light intensities. It becomes linear above about 300 μW/cm^2. This is qualitatively the same at all wavelengths we have investigated, namely in the near UV, the blue and the green range. The quantum yield was measured to be at least 0.8 for near UV and for blue light and at least 0.5 for green light, in the linear range.
4. The pH of maximum oxygen evolution depends on the composition of the system. For an AgCl layer with an excess of about 10^{-3} M Ag^+ it is at approximately pH 4. In case of AgCl on Ag^+–A zeolite it is around pH 6 and on mordenite it is in the alkaline region. This means that optimization for a specific application is feasible to a certain extent. In presence of a small excess of Cl^- the system becomes insensitive to day light while at a large excess chlorine evolution is observed under acidic conditions with substantial quantum yield and oxygen can be detected with low yield only under alkaline conditions.
5. We have recently carried out experiments at the gas/solid interface. No oxygen evolution was observed at $AgCl/Ag^+$ layers but significant oxygen signals and also self-sensitization were measured for AgCl deposited on Ag^+–A zeolite. The $AgCl/Ag^+$ layers become immediately very acidic so that only tiny amounts of oxygen can be formed while the buffering capability of the zeolite framework helps to maintain favourable conditions for the oxidation of water in $AgCl/Ag^+$–A zeolite samples [26].

Based on these observation we deduce a reaction mechanism of the photochemical O_2 evolution which takes into account the different behaviour of $AgCl/Ag^+$ and $AgCl/Cl^-$ [10].

- Light absorption proceeds via an LMCT transition in which an adsorbed silver atom and an adsorbed chlorine radical are formed at the surface. This can also be described as "electron–hole pair" formation. The chlorine radical can be understood as a surface species (s) and the silver atom can be understood as an interstitial (i) surface species.

- (A) $\mathrm{AgCl} + h\nu \xrightarrow{\text{charge transfer transition}} \mathrm{Ag}^{\bullet}_{s,i} + \mathrm{Cl}^{\bullet}_{s}$
- Any recombination is a loss process.
- Two radicals combine to form Cl_2. Chlorine evolution has been measured in a number of experiments, see e.g. [20,21].
- (B) $2\mathrm{Cl}^{\bullet}_{s} \rightarrow \mathrm{Cl_2}$

- At low pH Cl_2 is stable and can be collected. In less acidic conditions it reacts with water to form hypochloric acid.
- (C) $Cl_2+H_2O \rightleftarrows HOCl+H^+ +Cl^-$
- This reaction is supported by an excess of Ag^+ which captures the Cl^- and shifts the equilibrium to the right.
- (D) $Cl^- + Ag_s^+ \rightleftarrows AgCl_s$
- HOCl acid is a weak acid with a pK_a value of 7.58.
- (E) $HOCl+OH^- \rightleftarrows OCl^- + H_2O$
- HOCl and OCl^- are rather stable under many conditions. However, silver species catalyse the decomposition of HOCl to oxygen, protons and Cl^- according to:
- (F) $2HOCl \xrightarrow{Ag_+} O_2 + 2H^+ + 2Cl^-$
- Step (F) can be tested easily by adding some silver nitrate to a hypochloric acid solution of pH~5 which causes rapid oxygen evolution.
- The interstitial silver atoms form clusters of yet unknown size and charge according to equation (G), as can easily be observed by the colour change taking place.
- (G) $n\mathrm{Ag}^{\bullet}_{s,i} + m\mathrm{Ag}^+ \xrightarrow{\text{cluster growth}} [\mathrm{Ag}]^{m+}_{n+m}$
- These clusters act as colour centres, responsible for the self-sensitization [27].

Step (B) explains why, with acidic solutions and an excess of Cl^-, chlorine formation is observed, while step (F) explains the oxygen evolution in case of an excess of Ag^+ and at medium pH. At low light intensities, we observed a non-linear dependence of the O_2 evolution rate on the light intensity which changes into a linear dependence above about 300 $\mu W/cm^2$. Four redox equivalents have to be accumulated for the formation of one O_2 molecule. In the mechanism presented, this occurs in steps (B) and (F), where two partially oxidized species react with each other. It is reasonable to assume that recombination reactions play a more important role at low light intensities than at higher values, because the speed of step (B) depends crucially on the concentration of chlorine radicals. At low intensity the oxygen evolution rate is proportional to the square of the light intensity. The lifetime of the chlorine radicals can be estimated to be in the order of a few dozen micro seconds. This estimate is based on luminescence lifetime measurements. Above a critical light intensity the chlorine radical concentration is so high that losses become negligible.

It is satisfactory that the photocatalytic oxygen evolution on $AgCl/Ag^+$ systems can be explained as a sequence of simple one electron steps. The excess of Ag^+ needed for efficient oxygen evolution is due to a surface effect. The two different situations, excess of Ag^+ and excess of Cl^- in the system, can be sketched as shown in Fig. 3.

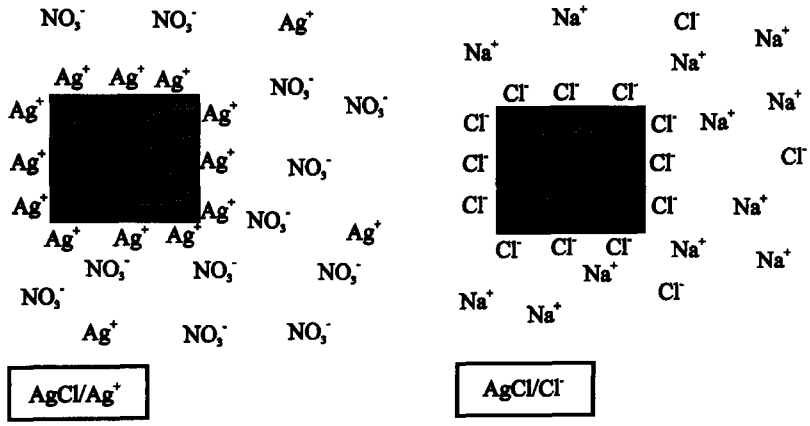

Fig. 3. Surface of AgCl for different concentrations of Ag^+ and Cl^- ions in the solution. Left: When Ag^+ is in excess the AgCl carries excess silver ions at its surface and the double layer is completed by the counter ion, nitrate; this is the $AgCl/Ag^+$ case. Right: When the halide ion is in excess the remaining AgCl adsorbs excess halide ions on its surface and a sheath of Na^+ ions completes the electrical double layer; this is the $AgCl/Cl^-$ case.

The reduced silver species must be oxidized to make the photochemical water oxidation useful for solar energy conversion.

$$[(n-r)\mathrm{Ag}^+, m\,\mathrm{AgCl}, r\,\mathrm{Ag}^0] \underset{\text{electrode}}{\overset{+r^{\oplus}}{\rightarrow}} [n\,\mathrm{Ag}^+, m\,\mathrm{AgCl}]$$

Recent photoelectrochemical experiments on Ag^+/AgCl layers on conduction SnO_2 and on other electrodes gave encouraging results in that simultaneous photocatalytic oxygen generation from water and oxidation of the reduced silver could be observed over many hours [11].

3. Zeolite microcrystals as hosts for supramolecular organization of clusters, complexes and molecules

Zeolite microcrystals can act as hosts for supramolecular organization of clusters, complexes and molecules, see e.g. [28–31]. They offer possibilities to design precise and reversible functionalities which have the potential to become useful in a solar energy conversion system because in favourable cases very stable materials have been obtained. The possibility to arrange zeolite microcrystals of good quality and narrow size distribution as dense monograin layers on different types of substrates allows us to achieve specific properties [32]. In the present context three functionalities are of special importance: intrazeolite ion transport, intrazeolite charge transport and intrazeolite excitation energy transport. All of them have been clearly demonstrated experimentally although there are still some controversies going on. The zeolite acts as a host in each case mentioned. It is not actively involved in the corresponding processes, but provides the necessary geometrical and chemical environment. One of the difficulties in this field is that the materials used are often poorly characterized and do not correspond to what the experimentalists assume to have in their hands [33,34]. The zeolite community has made it difficult for newcomers to synthesize or to obtain the material they need to have. But this unpleasant situation is improving rapidly.

Silver zeolite A is a good example to illustrate some difficulties, especially the appealing properties of such systems. It was assumed that the zeolite is important in the photochemical oxidation of water with visible light observed in Ag^+–A zeolite system. This turned out not to be the case in presence of liquid water [10,35] but the zeolite ion exchange properties were found to play an important role in experiments at the solid/gas interface, however, as discussed in Section 2 [26].

In situ spectroscopy on well-defined monograin layers and quantum chemical calculations on systems containing several hundred atoms have provided new insight. Rálek et al. [36] reported in 1962 that Ag^+–A zeolites turn from white over yellow to full yellow–red under dehydration at elevated temperature and that this colour change is reversible under rehydration. These colour changes were repeated and discussed by a number of authors and the explanations for their occurrence range from charge transfer interactions between the Ag^+ ions and the zeolite framework oxygen, responsible for the yellow colour, to multistep autoreductive processes involving framework oxygen and formation of partially reduced silver clusters. This discussion has been reviewed by Sun and Seff [37]. We have observed that the yellow colour can be observed by evacuating thin Ag^+–A zeolite layers at room temperature. After adding a little degassed water via the vacuum system, the samples turned to white again within a fraction of seconds. This was reproduced several times over three days and no permanent changes could be observed. Addition of dry oxygen to the yellow samples did not have any visible effect. Based on this information and on quantum chemical calculations we concluded that the yellow colour of the evacuated Ag^+–A zeolite layers can be attributed to an LMCT charge transfer from the zeolite framework oxygen to the silver ions and that the colour change can be described simply as a dehydration/hydration process of the Ag^+ in the zeolite [38]:

$$\underset{\text{colourless}}{\mathrm{A{-}Ag^+{-}(OH_2)_n}} \overset{\text{dehydration}}{\underset{\text{hydration}}{\rightleftarrows}} \underset{\text{deep yellow}}{\mathrm{A{-}Ag^+} + n\mathrm{OH_2}}$$

More detailed experimental and theoretical studies on Ag_n^{m+} clusters in the zeolite A cavities have lead to the interpretation explained in Fig. 4. In the upper part we see the development of the Ag(5s)-type levels of the silver species in a zeolite. The lowest and the highest Ag(5s)-type levels are shown. All of them are embedded between the HOMO region of the zeolite,

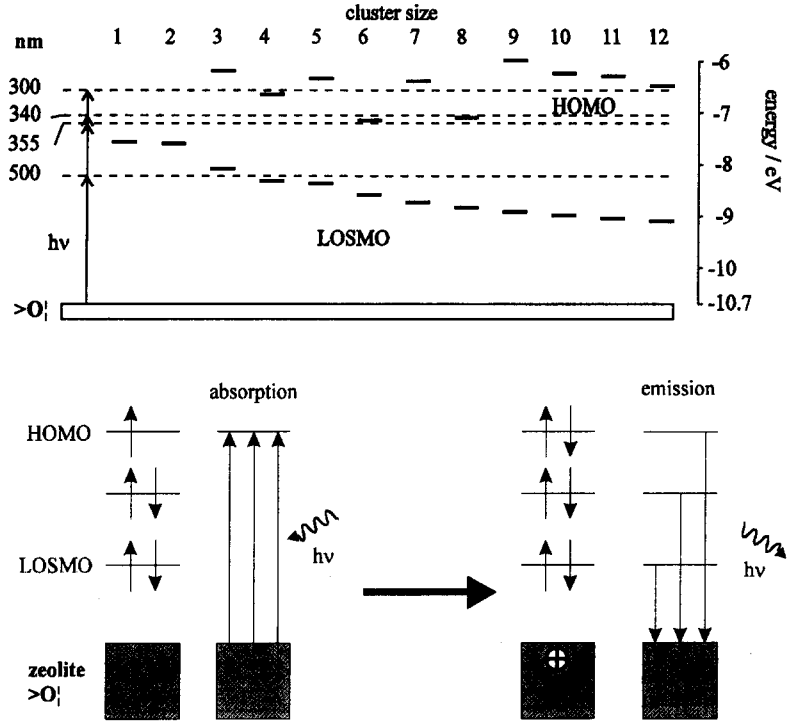

Fig. 4. Electronic structure and electronic absorption/emission processes in silver zeolites. Upper part: Development of the Ag(5s)-type levels of the silver species in a zeolite. The lowest and the highest Ag(5s)-type levels are shown. All of them are embedded between the HOMO region of the zeolite, which consists of oxygen lone pairs denoted as (>O|). The position of the different cluster-HOMOs are indicated by a dashed line. It depends on the size and on the charge of the clusters. The lowest Ag(5s)-type level, the LOSMO, plays a special role in the description of luminescence properties of such materials. Lower part: Absorption/emission properties of a distorted Ag_6^+ cluster embedded in a zeolite framework. An electron is injected into the cluster from the zeolite–oxygen lone pair region via an LMCT transition. Emission is of MLCT type. It can occur from all three doubly occupied Ag(5s)-type levels, the longest wavelength emission being a >O|←LOSMO transition.

which consists of oxygen lone pairs denoted as (>O|), and its LUMO region lying at −2–0 eV which is not shown. The Ag(5s)-type levels interact only weakly with levels belonging to the zeolite. The largest cluster in the α-cage of zeolite A consists of six silver atoms. The position of the cluster-HOMO depends on the charge of the cluster. It makes sense to name the lowest Ag(5s)-type level "lowest-s-molecular orbital" (LOSMO), because of the special role it plays in the description of luminescence properties of such materials due to its position and due to the weak interaction of the Ag(5s)-type level with the zeolite framework.

The lower part of this view graph illustrates absorption/emission properties of a distorted Ag_6^+ cluster embedded in a zeolite framework. An electron is injected into the cluster from the zeolite–oxygen lone pair region via an LMCT transition. Emission can occur from all three doubly occupied Ag(5s)-type levels, the longest wavelength emission being of >O|← LOSMO MLCT type. More details on these interesting observations will be published elsewhere [39].

Many different zeolite based materials have been reported. An interesting example is the $Ru(bpy)_3^{2+}-Y$ zeolite which was discussed by Dutta two years ago at a conference [31]. We have shown that up to about 60% of the supercages can be filled with this complex, by the known "ship-in-a-bottle" syntheses procedures [33]. Our result is illustrated in Fig. 5. At higher loading an increasing amount of by-products corresponding formally to $Ru(bpy)_n(NH_3)_{6-2n}^{3+}$, $n<3$, was found.

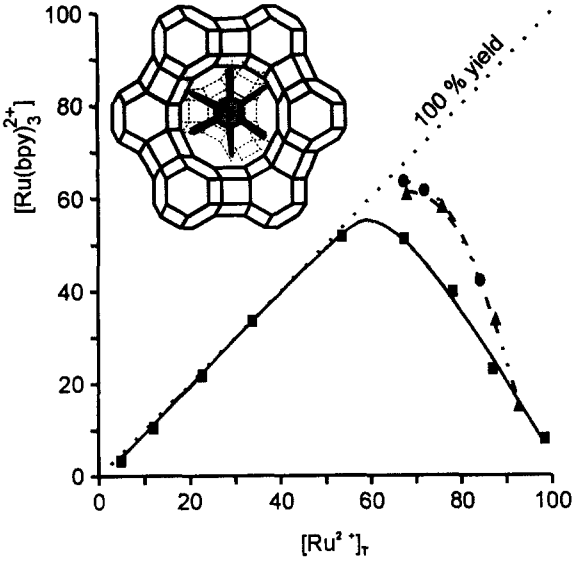

Fig. 5. Analysis data for zeolites at different loadings. The loading $[Ru(bpy)_2^{3+}]$ is drawn as a function of the total loading $[Ru^{2+}]_T$. A 100% value corresponds to a loading of one ruthenium/bpy complex per supercage. The samples at high loading were reacted with bpy a second time (triangles) and, in some cases, a third time (circles) [33].

Another interesting material which has been investigated by us and others is MV^{2+} in Zeolite Y. This is the easiest case known so far to demonstrate intrazeolite charge transfer because a very pronounced and easy to understand dependence of the cyclic voltammograms on the electrolyte cations was observed [40].

Very different systems are obtained by intercalating strongly luminescent organic dyes into the nanopores of hexagonal zeolites with channel structure. We discuss them in the next section.

4. Energy transfer between dye molecules in the channels of hexagonal microporous crystals

From the natural antenna we deduce that highly concentrated monomeric dye molecules with a large Förster energy transfer radius and a high luminescence quantum yield in an ideal geometrical arrangement of optimal size are favourable conditions for realizing an efficient device as illustrated in Fig. 2. Dyes in high concentration usually have the tendency to form aggregates which in general show very fast radiationless decay. In natural antenna systems the formation of aggregates is prevented because the chlorophylls are fenced in polypeptide cages [41]. A similar approach is possible by enclosing dyes inside of a microporous material such that the volume of the cages and channels is able to uptake monomers only but not aggregates. Materials bearing linear channels running through a whole microcrystal allow the formation of highly anisotropic dye assemblies. Zeolites having such channels, large enough to uptake organic dye molecules, are especially attractive. Examples of such zeolites can be found in [42]. A few cases based on zeolite L as a host and the cationic dye molecules pyronine and oxonine have been investigated experimentally to some extent for this purpose. Intercalation of thionine in zeolite L was found to be useful for learning about space filling properties and about isothermal ion exchange relevant in these studies [43]. Space filling models show that while the molecules can penetrate the channels, formation of dimers inside of them is not possible. The synthesis of zeolite L microcrystals with sizes ranging from 20 nm to 1 μm and with cylinder morphology and varying length to diameter ratio ranging from a disc to a cigar-like shape has recently been reported [44,45].

Gfeller and Calzaferri [12] have carried out a theoretical study on energy transfer, energy migration, and trapping efficiencies of systems related to that illustrated in Fig. 2. The basic assumptions used in these investigations can be summarized as follows. The antenna is built by dye molecules in hexagonally arranged linear channels as illustrated in Fig. 6. The primitive vector $\boldsymbol{c}$ corresponds to the channel axis while the primitive vectors $\boldsymbol{a}$ and $\boldsymbol{b}$ are perpendicular to it enclosing an angle of 60°. The channels run parallel to the central axis of the cylinder. The length and radius of the cylinder are l_{cyl} and r_{cyl}, respectively. The theory is based on a few assumptions which are supported by experiments carried out on cationic dye molecules in zeolite L. The description of the processes is simplified by referring to a large number of microcrystals with a narrow distribution of size and shape.

A 0.1 μm large zeolite L microcrystal with equal length and diameter ($l_{cyl}=2\times r_{cyl}$) contains about 750 parallel channels. Each channel consists of 134 unit cells. Dye molecules with a size like pyronine and oxonine occupy two unit cells ($u=2$). This means that

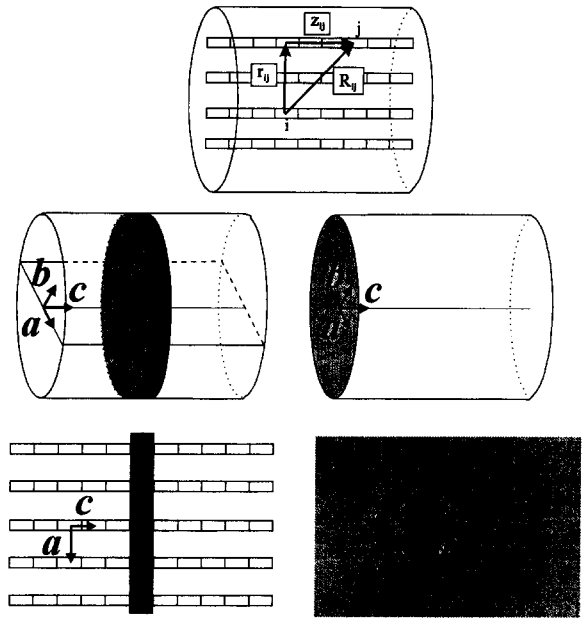

Fig. 6. Geometrical arrangement of the antenna. The sites are marked by rectangles.Top: Definition of the distances R_{ij}, r_{ij} and z_{ij} between sites i and j. Left: Cut through the centre of the cylindrical microcrystal along a and c. The sites of the shaded area belong to one slab. Right: Cut vertical to c. The channels indicated by circles are arranged in rings around the central channel as a consequence of the hexagonal symmetry [12].

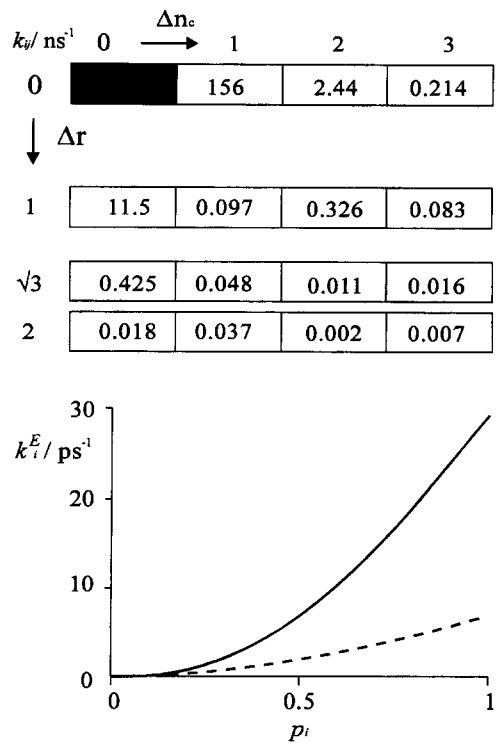

Fig. 7. Rate constants for different situations. Top: Energy transfer rate constants k_{ij} in units of 10^9 s^{-1}, for jumps from the shaded site i to neighbour sites j for p_i=0.25 and J_{ij} =1.05×10^{-3} cm^3 M^{-1} Bottom: Depopulation rate constant k_i^E (ps^{-1}) of a site i as a function of the occupation probability p_i for J_{ij}=4.4×10^{-13} cm^3 M^{-1} (solid) and for J_{ij}=1.05×10^{-13} cm^3 M^{-1} (dashed).

up to 67 dye molecules find place in one channel. Such a microcrystal can contain up to 50 250 dye molecules. An impression on the rate of energy migration in such a system is provided in Fig. 7. It contains two kinds of information. We show in the upper part individual rate constants k_{ij} from the starting site which is shaded to a representative selection of neighbour sites and in the lower part the energy migration constant k_i^E as a function of the occupation probability p_i. Energy transfer to the nearest neighbours along the channel axes is by far the most probable event. With increasing distance z_{ij} the individual rate constants k_{ij} for energy transfers decrease strongly. The reason for this is the pronounced distance dependence of the dipole–dipole interactions. Energy transfer to the nearest neighbours perpendicular to the channel axes is much less probable than along the channel axes. This difference is caused mainly by the orientation factor, which is strongly different for this two transitions, and not so much by the only slightly larger distance. We observe for the same reason that the rate constant for the transition along the vector (Δn_a, Δn_c)=(1,1) is much smaller than along the vector (Δn_a, Δn_c)=(1,2), although the distance for the latter transition is larger.

All rate constants k_{ij} are proportional to the square of the occupation probability p_i^2 and to the spectral overlap J_{ij}. The ratio between the different rate constants is therefore not affected by these parameters and any sum of rate constants k_{ij} shows the same proportionalities. The square dependence on the occupation probability of the energy migration constant k_i^E, which is the sum of the rate constants k_{ij} of energy transfers from site i to any site j of the microcrystal, is documented in the lower part of Fig. 7. Its value is significantly larger than 0.2 ps^{-1} even at rather low occupation probabilities p_i. The energy migration constant in the antenna system of green photosynthetic bacterium *Chloroflexus aurantiacus* was reported to be 0.2 ps^{-1} [46].

Table 1
Front trapping efficiency $T_{F,\infty}$ and fluorescence quantum yield Φ_F for different cylinder lengths l_{cyl}, two different occupation probabilities p_i and two different spectral overlaps J_{ij} [12]

l_{cyl} (nm^{-1})	p_i	$J_{ij}=1\times10^{-13}$ cm^3 M^{-1}		$J_{ij}=4\times10^{-13}$ cm^3 M^{-1}	
		$T_{F,\infty}$	Φ_F	$T_{F,\infty}$	Φ_F
50	0.25	0.62	0.38	0.86	0.14
100		0.35	0.65	0.64	0.36
150		0.23	0.77	0.48	0.53
200		0.17	0.83	0.38	0.62
250		0.14	0.86	0.31	0.69
50	1	0.96	0.04	0.99	0.01
100		0.87	0.13	0.96	0.04
150		0.77	0.23	0.93	0.07
200		0.69	0.31	0.9	0.1
250		0.62	0.38	0.86	0.14

Energy migration along the channel axes can be expressed as energy transfer from one slab to another. Analogously, energy migration perpendicular to it can be expressed as energy transfer between the channels. The rate constants reported in Fig. 7 for transitions between slabs, kz_{ij}, and between channels, kr_{ij}, have been calculated for the same occupation probability and the same spectral overlap as used for Fig. 7 (top). The rate constants between slabs are symmetrical, which means $kz_{ij}=kz_{ji}$, and the kr_{ij} are the same for all channels sitting on the same circle around the shaded channel. Energy transfer to the next neighbour slabs is about 18 times more probable than to any other slabs. The rate constant for transitions between neighbour slabs is close to that for transitions between neighbour sites inside one channel. This means that energy migration along the channel axes runs predominantly inside the same channel simply from one site to its nearest next neighbour. Energy migration perpendicular to the channel axes is much slower. It occurs predominantly between nearest next neighbour sites inside the same slab.

We have shown that it is convenient to distinguish between different types of trapping [12]. They are named according to the position of the traps: *Front trapping* $T_F(t)$ refers to traps positioned only on the front side of the cylindrical microcrystals. Thus, they are found in the slab $n_c=0$. *Front–back trapping* $T_{FB}(t)$ refers to traps on the front and to traps on the back positioned in the slab $n_c=0$ and $n_c = n_c^{max}$, respectively. *Coat trapping* $T_C(t)$ refers to traps positioned on the coat of the cylinder, this means in the outermost channels having a distance to the central channel between $r_{max}-|a|$ and r_{max}. *Axial trapping* $T_A(t)$ refers to traps located in the central channel. Finally, *point trapping* $T_P(t)$ refers to a single trap positioned at the centre of the front side. All these trapping types reflect symmetry aspects of the cylinder investigated. Front–back trapping and front trapping are governed by energy migration along c while coat trapping and axial trapping are governed by energy migration perpendicular to it. Point trapping depends on both directions of energy migration.

An important result we have obtained is summarized in Table 1 where the *front trapping efficiency* $T_{F\infty}$ observed at infinite time after the excitation of a dye in the antenna is reported as a function of the size of the microcrystal for two different occupation probabilities and two spectral overlaps. It shows that nearly quantitative trapping efficiencies are feasible in a well-designed system.

5. Conclusions

We have focused on three problems: the photocatalytic water oxidation in absence of an externally added potential, the charge transport in an organized microporous media and the transport of excitation energy in an antenna system [47].

It is satisfactory that the very efficient photocatalytic oxygen evolution on AgCl/Ag$^+$ systems can be

explained as a sequence of simple one electron steps. The excess of Ag^+ needed for efficient oxygen evolution is a surface effect. The reduced silver species must be oxidized to make the photocatalytic water oxidation useful for solar energy conversion. It is not difficult to reoxidize the photochemically produced Ag^0 completely to Ag^+. It is, however, difficult to design a completely reversible and stable system. Recent photoelectrochemical experiments on Ag^+/AgCl layers on conduction SnO_2 and other electrodes gave encouraging results in that simultaneous photochemical oxygen generation from water and oxidation of the reduced silver could be observed over many hours.

Zeolite microcrystals can act as hosts for supramolecular organization of clusters, complexes and molecules. They offer possibilities to design precise and reversible functionalities which have the potential to become useful for solar energy conversion. Arranging zeolite microcrystals as dense monograin layers of good quality on different types of substrates allows us to achieve specific properties. Three functionalities are of special importance: intrazeolite ion transport, intrazeolite charge transport and intrazeolite excitation energy transport. The zeolite acts as a host in each case.

Favourable conditions for an antenna device are highly concentrated monomeric dye molecules with a large Förster energy transfer radius and a high luminescence quantum yield in an ideal geometrical arrangement of optimal size. This can be realized by enclosing dyes inside of a microporous material in a way that the volume of the cages and channels is able to uptake monomers only but not aggregates. Zeolites bearing linear channels running through a whole microcrystal allow the formation of highly anisotropic dye assemblies. We have found that they can lead to nearly quantitative trapping efficiencies.

Acknowledgements

This work is part of project NF 20-046617.96/1, financed by the Schweizerischer Nationalfonds zur Forderung der wissenschaftlichen Forschung and project BEW (93)034, financed by the Swiss Federal Office of Energy.

References

[1] V. Balzani, S. Campagna, G. Denti, A. Juris, S. Serroni, M. Venturi, Solar Energy Mater. Sol. Cells 38 (1995) 159.
[2] H. Bücher, K.H. Drexhage, M. Fleck, H. Kuhn, D. Möbius, F.P. Schäfer, J. Sondermann, W. Sperling, P. Tillmann, J. Wiegand, Mol. Crystals 2 (1967) 199.
[3] H. Tributsch, Proc. IPS-10, in: Z.W. Tian, Y. Cao (Eds.), International Academic Publishers, Beijing, 1993, p. 235.
[4] C.A. Bignozzi, R. Argazzi, J.R. Schoonover, G.J. Meyer, F. Scandola, Solar Energy Mater. Sol. Cells 38 (1995) 187.
[5] E. Amouyal, Solar Energy Mater. Sol. Cells 38 (1995) 249.
[6] A.J. Bard, M.A. Fox, Acc. Chem. Res. 28 (1995) 141.
[7] R. Beer, F. Binder, G. Calzaferri, Photochem. Photobiol. A 69 (1992) 67.
[8] G. Calzaferri, S. Hug, T. Hugentobler, B. Sulzberger, Photochem. Photobiol. A 26 (1984) 109.
[9] B. Sulzberger, G. Calzaferri, Photochem. Photobiol. A 19 (1982) 321.
[10] K. Pfanner, N. Gfeller, G. Calzaferri, J. Photochem. Photobiol. A 95 (1996) 175.
[11] M. Lanz, G. Calzaferri, J. Photochem. Photobiol. A 109 (1997) 87.
[12] N. Gfeller, G. Calzaferri, J. Phys. Chem. 101 (1997) 1397.
[13] P.J. Riggs-Gelasco, R. Mei, CH.F. Yocum, J.E. Penner-Hahn, J. Am. Chem. Soc. 118 (1996) 2387.
[14] K. Wieghardt, Angew. Chem. 106 (1994) 765.
[15] L.J. Schaaf, Out of the Shadows: Herschel, Talbot and the Invention of Photography, Yale University Press, New Haven, CT, 1992.
[16] G. Calzaferri, N. Gfeller, K. Pfanner, J. Photochem. Phototbiol. A 87 (1995) 81.
[17] M.J. Ware, IS and T's 48th Annual Conference Proceedings, Washington DC, 7–11 May, 1995, p. 86.
[18] E. Baur, A. Rebmann, Helv. Chim. Acta 4 (1921) 256.
[19] H. Vogel, Ann. Phys. 119 (1863) 497.
[20] G. Calzaferri, W. Spahni, J. Photochem. Photobiol. A 32 (1986) 151.
[21] R. Beer, G. Calzaferri, W. Spahni, Chimia 42 (1988) 134.
[22] H. Metzner, K. Fischer, Photosynthetica 8 (1974) 257.
[23] H. Metzner, K. Fischer, G. Lupp, Photosynthetica 9 (1975) 327.
[24] K. Chandrasekaran, J.K. Thomas, Chem. Phys. Lett. 97 (1983) 357.
[25] H. Taube, W.C. Bray, J. Am. Chem. Soc. 62 (1940) 3357.
[26] F. Saladin, I. Kamber, K. Pfanner, G. Calzaferri, J. Photochem. Photobiol. A 109 (1997) 47.
[27] G. Calzaferri, in: Z.W. Tian, Y. Cao (Eds.), Proceedings of the Ninth International Conference on Photochemical Conversion and Storage of Solar Energy, IPS-9, International Academic Publishers, Beijing, 1993, pp. 141–157.
[28] D. Wöhrle, G. Schulz-Ekloff, Adv. Mater. 6 (1994) 875.
[29] J. Caro, F. Marlow, M. Wübbenhorst, Adv. Mater. 6 (1994) 413.
[30] F. Schüth, Chemie i.u. Zeit 29 (1995) 42.
[31] P.K. Dutta, M. Borja, M. Ledney, Sol. Energy Mater. Sol. Cells 38 (1995) 239.

[32] P. Lainé, R. Seifert, R. Giovanoli, G. Calzaferri, New J. Chem. 21 (1997) 453.
[33] P. Lainé, M. Lanz, G. Calzaferri, Inorg. Chem. 35 (1996) 3514.
[34] B.R. Müller, G. Calzaferri, J. Chem. Soc., Faraday Trans. 92 (1996) 1633.
[35] G. Calzaferri, in: R. Corriu, P. Jutzi (Eds.), Proceedings Taylor-Made Silicon–Oxygen Compounds, From Molecules to Materials, Bielefeld, 3–5 September, 1995, pp. 149–169.
[36] M. Rálek, P. Jiru, O. Grubner, H. Beyer, Collect. Czech. Chem. Commun. 27 (1962) 142.
[37] T. Sun, K. Seff, Chem. Rev. 94 (1994) 857.
[38] G. Calzaferri, A. Kunzmann, P. Lainé, K. Pfanner, IS and T's 48th Annual Conference Proceedings, Washington, DC, 7–11 May, 1995, p. 318.
[39] R. Seifert, A. Kunzmann, G. Calzaferri, to be published.
[40] G. Calzaferri, M. Lanz, J.W. Li, J. Chem. Soc., Chem. Commun. (1995) 1313.
[41] W. Kühlbrandt, D.N. Wang, Nature 350 (1991) 131.
[42] M.W. Meier, D.H. Olson, Atlas of Zeolite Structure Types, Butterworths, Stoneham, MA, 1988.
[43] G. Calzaferri, N. Gfeller, J. Phys. Chem. 96 (1992) 3428.
[44] S. Ernst, J. Weitkamp, Catal. Today 19 (1994) 27.
[45] M. Tsapatsis, O. Tatsuya, M. Lovallo, M.E. Davis, Mat. Res. Soc. Symp. Proc. 371 (1995) 21.
[46] S. Savikhin, Y. Zhu, R.E. Blankenship, W.S. Struve, J. Phys. Chem. 100 (1996) 3320.
[47] G. Calzaferri, Sol. Energy Mater. Sol. Cells, in press.